Dynamic single cell culture array†‡

Dino Di Carlo, Liz Y. Wu and Luke P. Lee*

Received 26th April 2006, Accepted 16th August 2006
First published as an Advance Article on the web 4th September 2006
DOI: 10.1039/b605937f

It is important to quantify the distribution of behavior amongst a population of individual cells to reach a more complete quantitative understanding of cellular processes. Improved high-throughput analysis of single cell behavior requires uniform conditions for individual cells with controllable cell–cell interactions, including diffusible and contact elements. Uniform cell arrays for static culture of adherent cells have previously been constructed using protein micropatterning techniques but lack the ability to control diffusible secretions. Here we present a microfluidic-based dynamic single cell culture array that allows both arrayed culture of individual adherent cells and dynamic control of fluid perfusion with uniform environments for individual cells. In our device no surface modification is required and cell loading is done in less than 30 seconds. The device consists of arrays of physical U-shaped hydrodynamic trapping structures with geometries that are biased to trap only single cells. HeLa cells were shown to adhere at a similar rate in the trapping array as on a control glass substrate. Additionally, rates of cell death and division were comparable to the control experiment. Approximately 100 individual isolated cells were observed growing and adhering in a field of view spanning $\sim$1 mm^2 with greater than 85% of cells maintained within the primary trapping site after 24 hours. Also, greater than 90% of cells were adherent and only 5% had undergone apoptosis after 24 hours of perfusion culture within the trapping array. We anticipate uses in single cell analysis of drug toxicity with physiologically relevant perfused dosages as well as investigation of cell signaling pathways and systems biology.

Introduction

There is much interest in quantifying the range of biological responses of individual cells to various physiologically-relevant stimuli as opposed to bulk averages.[1,2] Once the distribution of responses to a stimulus have been characterized, this data can then be used in quantitative predictions of cell behavior in varied situations.[1] Particularly useful information can be acquired if the environmental factors that contribute to variable responses for individual cells are controlled.

One factor that may contribute to large distributions in behavior is cell–cell interactions between cells grown in a monolayer culture environment. Both contact and diffusible elements may play a role in this situation. Perfusion culture has been previously used and can reduce the effects of diffusible elements on cell behavior by convecting away produced substances that may provide autocrine or paracrine signals.[3–5] Perfusion, however, does not effect randomness introduced by cell–cell contact and communication through junctional proteins,[6] lipid nanotubes,[7] and membrane-bound-receptor to membrane-bound-ligand interactions.[8] Isolated cells in a monolayer culture can be observed to remove cell–cell contact contributions but this does not address diffusible elements. An additional problem is the nonuniformity of environment across the culture dish or well. For example, regions of high cell density may have reduced nutrients and higher waste concentrations than regions of sparse cell seeding. To address these problems arrayed uniform environments can be provided to culture cells and allow easy comparison of data between cells without confounding factors. Ideally, both secreted and contact signals can be controlled in these cases.

One widely used method of controlling contact signals and providing uniform seeding is done by micropatterning of the substrate and seeding cells on these controlled patches of extracellular matrix (ECM).[3,9–20] Most recently, this technique was used to study how cell cytoskeletal distribution effects cell division axis in hundreds of cells.[9] High density arrays of individual adherent cells can be created using these techniques.[13,15,21] Other methods have also been demonstrated for isolating arrays of single cells, without cell culture following.[22–24] The secreted microenvironment is not controlled using protein micropatterning or other array techniques alone however, but requires some method of dynamic perfusion control.

Large scale perfusion systems that do not recirculate media consume large quantities of reagents, so as expected microfluidic perfusion for cell culture has gained much attention. Perfusion culture in microfluidic devices has been demonstrated for large groups of cells[25–34] or individual cells[27] but not for ordered arrays. Takayama *et al.*[28–30] demonstrated a computer-controlled system based on Braille displays to provide perfusion to cells growing randomly on surfaces in a microfluidic device. Additionally, Jeon *et al.*[33,34] and Folch *et al.*[32] demonstrated patterned cell culture within a

Berkeley Sensor and Actuator Center, Biomolecular Nanotechnology Center, Department of Bioengineering, University of California, Berkeley, CA, 94720

† Electronic supplementary information (ESI) available: Cell division and apoptosis off-chip (figures) and a single cell culture under constant perfusion (video). See DOI: 10.1039b605937f

‡ The HTML version of this article has been enhanced with colour images.

microfluidic device, with continuous perfusion applied. In most cases, multicellular patterns of cells were formed on the modified surfaces. To multiplex several perfusion conditions for a single experiment, Voldman *et al.*[31] developed a logarithmically perfused microfluidic system and determined differences in morphology and growth characteristics for mouse embryonic stem cells and fibroblasts seeded randomly in the device. Both shear stress differences and differences in nutrient supply and convection of diffusible elements may play a role in the varied behavior observed.

In contrast to the above techniques, here we present a technique for both ordered single cell array formation and culture of an adherent cell line without chemical treatments of surfaces. Previously, we have shown single cell isolation and enzyme kinetic analysis using this platform,[35] but did not show maintenance of adherent cells and their behavior over long time periods. This technique allows dynamic microfluidic control of perfusion with uniform environments for individual cells. Cells within the trapping structures are also shielded from the higher shear stress in the main flow. The device is easily operated, with single cells loaded in arrays in less than 30 seconds.

Materials and methods

Microfluidic chip fabrication

The molds for the trapping array culture device were fabricated using negative photoresists (SU-8 50 and SU-8 2002, Microchem Corporation, 3000 rpm spin speed, 40 μm and 2 μm thick) as in Di Carlo *et al.*[36] Poly-dimethylsiloxane (PDMS, Sylgard 184, Dow Corning) was prepared according to the manufacturers instructions, degassed in a vacuum chamber for 1 hour and then poured on the mold and cured in a 70 °C oven for 2 hours. The PDMS was cut from the mold with a surgical scalpel and then carefully peeled off the mold. The fluid inlet and outlet were punched by a flat-tip needle for tube connections. Both a glass slide and the PDMS structures were treated with oxygen plasma (0.5 Torr, 40 W) for 20 seconds before bonding.

Cell culture and preparation

HeLa (human cervical carcinoma) cell line was used in experiments (American Type Culture Collection, Bethesda, MD). The cells were maintained by passaging twice weekly with Dubelcco's Modified Eagle Medium (DMEM) supplemented with 10% fetal bovine serum (FBS). For loading, adherent cells were detached from 100 mm diameter culture dishes with 5 mL trypsin EDTA (0.25%, Gibco, Carlsbad, CA). An equal amount of DMEM + FBS was then added to deactivate remaining trypsin. Cells were then centrifuged to a pellet and resuspended in phosphate buffered saline pH 7.4 (PBS, Gibco, Carlsbad, CA). A key experimental detail is to trap suspended cells within 15 minutes of trypsinization to reduced non-specific adhesion to surfaces. Freshly suspended cells were introduced into previously PBS filled devices by a syringe connected to a three way valve. For control experiments, suspended cells were introduced onto a glass slide contained by a PDMS well and cultured in either an incubator or (37 °C) heated stage for time-lapse experiments.

On-chip cell culture

Tubing, valves and devices were first sterilized with 70% ethanol for 5 minutes prior to loading. Sterile PBS was then used to prime the device and tubing. The previous steps were all done within a biosafety hood to reduce contamination. Then, cell solution was added and cells trapped to the desired density. Next, a valve was switched to sterile media + 10% FBS and flow was initiated to perfuse the cells. A flow rate of 0.75 μl min^{-1} using a syringe pump (Cole-Parmer) yielded an average velocity of $\sim$25 μm s^{-1} in the trapping region. Cells were either maintained in an incubator between images, or were heated to 37 °C on a microscope stage for time-lapse experiments.

Microscopy and data analysis

For time-lapse experiments an Olympus MIC-D microscope was outfitted with a heated stage. Time-lapse images were collected using the provided MIC-D software every 3 to 6 minutes. Images were analyzed to determine morphology and cell division using IrfanView. Cells with a long axis 1.3 times the short axis were considered to be "adherent". Cells were identified as dividing if they retracted from adherent morphology, became spherical and then separated into two daughter cells (see Fig. S1†). Cells were identified as apoptotic if they showed blebbing, no movement or shape change over 6 hours, or other apoptotic characteristics seen in Fig. S2.†

Device modeling

For cell culture it is important to understand and control the shear stress on cell surfaces, since cell pathways can be activated by high shear stress leading to unwanted cell behavior.[37] For our device the flow fields around an isolated trapping structure were modeled in 3D using the finite element method (FEMLAB 3.0, Comsol Inc.). The Navier–Stokes equations were used to model fluid flow with only viscous terms (*i.e.* $\rho = 0$ in the subdomains). Boundary conditions consisted of an average velocity of 25 μm s^{-1} at the inlet and pressure set to 0 at the outlet. The side walls of the computational domain were set to symmetry, simulating a row of trapping structures. A single trap (coarse mesh) was simulated instead of an array because an array became too computationally intensive to successfully solve with our current computational resources. Both velocities throughout the domain and shear stress components at the boundaries of the domain were collected.

Results and discussion

Single cell trapping arrays

Trapping arrays were successfully fabricated and tested. The device consists of branched trapping chambers linked in parallel (Fig. 1A), while the arrays within the chambers consist of U-shaped PDMS structures that are 40 μm in height and are offset from the substrate by 2 μm (Fig. 1B–C). Each chamber contained between 4 and 5 traps over its width (Fig. 1C). Also, each row of traps was asymmetrically offset from the previous row (Fig. 1C). It was qualitatively observed that asymmetric

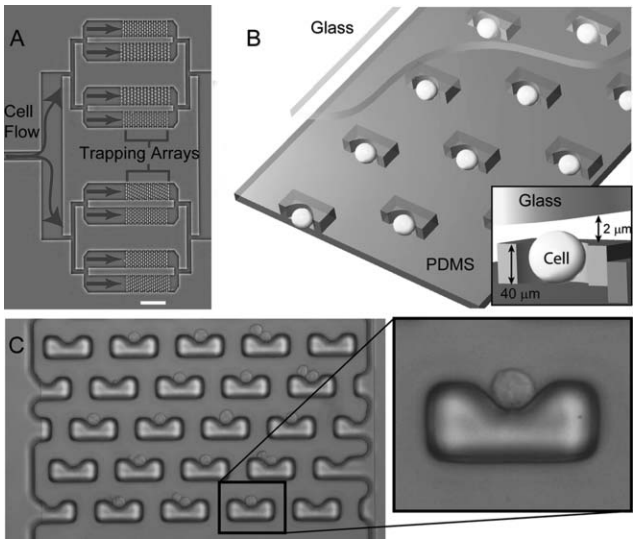

Fig. 1 Single cell trapping arrays. (A) A photograph of the cell trapping device is shown demonstrating the branching architecture and trapping chambers with arrays of traps. The scale bar is 500 μm. Cell and media flow enters from the left and enters the individual trapping chambers where it is distributed amongst the individual traps. (B) A diagram of the device and mechanism of trapping is presented. Traps are molded in PDMS and bonded to a glass substrate. Trap size biases trapping to predominantly one or two cells. The diagram is flipped from the actual device function for clarity; a functioning device is operated with the glass substrate facing down towards the earth. An inset shows the geometry of an individual trap. The device is not drawn to scale. (C) A high resolution brightfield micrograph of the trapping array with trapped cells is shown. In most cases cells rest at the identical potential minimum of the trap, while in some cases two cells are trapped in an identical manner amongst traps. A magnification shows the details of the trapped cell. Trapping is a gentle process and no cell deformation is observed for routinely applied pressures.

rows of traps were better at filling throughout the chamber when compared to symmetrically offset rows. Several lengths for the depth of the trap were examined for the best isolation of individual cells (10 μm, 15 μm, 30 μm, and 60 μm). It was found that ten micrometre deep traps most consistently trapped individual HeLa cells (average diameter $\sim$15 μm).[35] For other cell types with different average diameters, the optimum trap size should vary. Additionally, since there is a distribution of cell sizes amongst a population, there may be a bias to trap smaller cells that can more easily occupy the trapping sites.

Model of flow and shear stress in trap structures

The fluid velocity and shear stress were simulated as described in 'Materials and methods' for a single 3D trap structure containing a spherical trapped cell. This was conducted to determine shear stress conditions for trapped cells, to compare to physiologically relevant shear stresses. For a flow rate of 0.75 μL min^{-1} used in experiments the maximum velocity reaches $\sim$50 μm s^{-1} and the distribution of velocity magnitudes around a single occupied trap is shown in Fig. 2A at a position z = 20 μm from the substrate in the middle of the channel. In the region in front of and behind the trap the velocity is reduced as is expected. Shear stresses on a spherical trapped cell were also modeled and the distribution is plotted over the trapped cell and on the bottom surface of the channel for the same flow conditions (Fig. 2B). The shear stress of the bottom surface approximates that which an adherent cell would feel. Here, the average shear stress, observed outside the trapping structure is 6×10^{-2} dyn cm^{-2} and the average shear stress in the trap is 2.5×10^{-3} dyn cm^{-2}. This leads to a ratio of shear stress between the main flow and within the trap of $\sim$24. The average shear stress on a spherical trapped cell is also 3.5×10^{-3} dyn cm^{-2}. These numbers are much below physiological shear stress of $\sim$10 dyn cm^{-2} that vascular endothelial cells experience but comparable to shear stress caused by interstitial flow.[38] The shear stress ratio observed in our device will remain independent of flow rate for low Reynold's number and is a number characterizing how "shielded" the trapped single cells will be from the main flow.

Arrayed single cell culture

We demonstrate culture of ordered arrays of single HeLa cells under constant perfusion of media + 10% FBS. For a flow rate of 25 μL min^{-1} time-lapse images were taken every 3 minutes of a trapped array of HeLa cells on an incubated microscope stage (Fig. 3). Cells are shown after 12 and 24 hours in Fig. 3B–C. Initially, the single cell trapping rate for this sequence was 70% (Fig. 3A). After 12 hours small changes in morphology are observed away from a spherical morphology towards an adherent morphology. Also, cell division is observed in a few cases (top arrow – Fig. 3B). After 24 hours, a majority of cells display an adherent morphology and both cells identified with arrows have divided. In some cases cells are observed to escape the trapping structures as well. Behavior of several cells in the trapping structure over time is shown for dividing and adhering cells in Fig. 4. It should be noted that in most cases after cell division both daughter cells

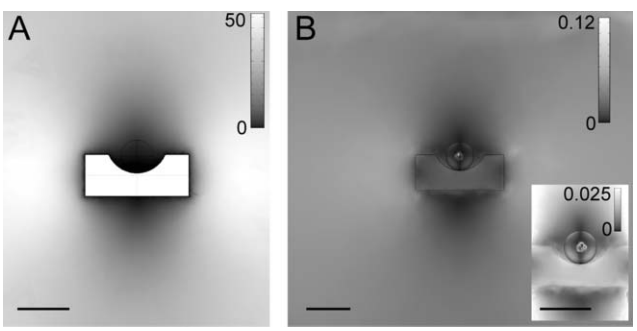

Fig. 2 Modeling shear stress. Velocity magnitude and shear stress magnitude is plotted for a 3D model of the trapping structure with a trapped spherical cell. Velocity magnitude is plotted for a z distance 20 μm from the substrate, while shear stress magnitude is plotted for the boundary surface of the microchannel and trapped cell. (A) Velocity magnitude is plotted showing a region of reduced velocity within the trapping structure. The scale goes from a maximum of 50 μm s^{-1} to a minimum of 0 μm s^{-1}. (B) Shear stress magnitude is plotted on the lower boundary of the device. Here the scale extends from 0 to 0.12 dyn cm^{-2} in the main graph. An inset shows a close-up of the trapping region with a new scale extending from 0 to 0.025 dyn cm^{-2}. Notice the reduced shear stress within the trapping structure. Scale bars are 25 μm.

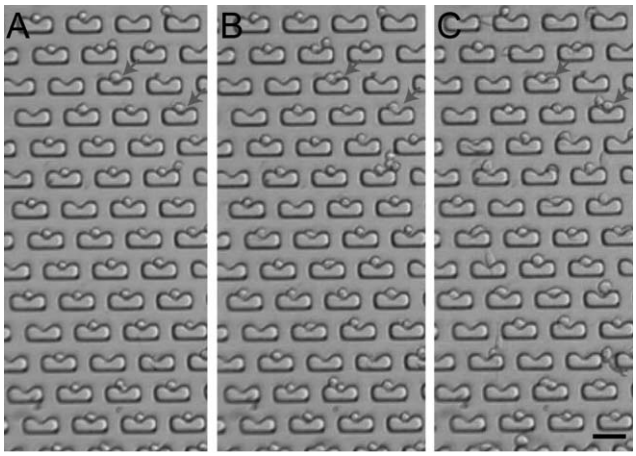

Fig. 3 Arrayed single cell culture. Micrograph images of cells cultured within the microfluidic arrays are shown. Cells were cultured under continues perfusion of media + 10% FBS with an average velocity (25 μm s^{-1}) for over 24 hours (Video S1†). Pictures are shown at times (A) 0 h, (B) 12 h, and (C) 24 h. The arrows indicate cells that undergo cell division within this time period. Scale bar is 50 μm.

remain isolated in the trapping structure. Another interesting observation is the directionality of adherence in HeLa cells that are trapped. It is observed that a large fraction of growing HeLa cells have a long axis parallel to the long axis of the trapping structure. It also appears that the cells became adherent to the PDMS structure as opposed to the glass substrate in these cases. This may be due to serum containing adhesion-promoting proteins that may adhere to the hydrophobic PDMS surface biasing attachment. Adhesion on the PDMS structures may limit microscopic analysis in some cases, due to diffraction at the interface of the trap. To limit

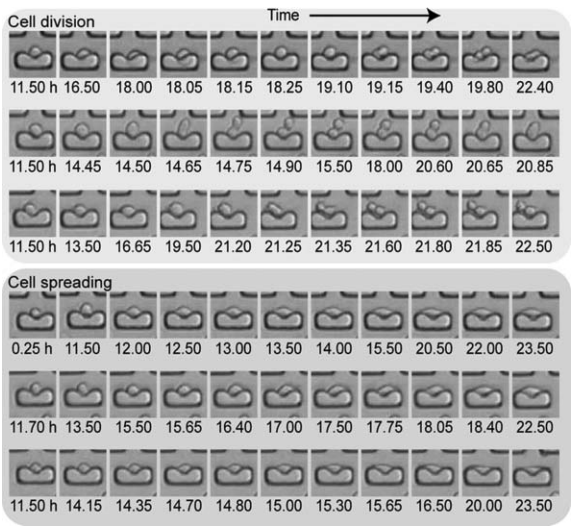

Fig. 4 Uniform cell behavior. Characteristics of growth for single trapped cells are shown. Frames from a movie of cell growth in the array are shown demonstrating both cell division (first three rows) and morphologies indicative of cell adhesion (rows 4 through 6). Notice the uniformity in morphology observed amongst adherent and amongst dividing cells. The hours after seeding are shown underneath each image. After division daughter cells remained within the trapping region.

adhesion, future studies could employ treatments with high concentrations of bovine serum albumin (BSA) that will coat the PDMS surface.

Quantitative analysis of the dynamics of cell adhesion, death, division, and escape from traps were performed for a 24 hour period (Video S1†) and are plotted in Fig. 5A. Here it was observed that 50% of cells displayed adherent morphology after 15 hours. After 24 hours 6% of cells showed characteristics of apoptosis, while 15% had escaped from the vicinity of the initial trapping site. The high level of maintenance within the trapping structures after 24 hours may be due to shear sheltering within the trapping structure. Additionally, 5% of cells had undergone cell division after 24 hours. These results were compared to cell behavior in a control experiment using the same glass substrate with no traps or perfusion (Fig. 5B). In this experiment 50% of cells were adherent after a similar 14 hours, while 5% of cells were apoptotic after 24 hours, and only 1% of cells had undergone cell division. Typical behavior of dividing cells and apoptotic cells as observed in the control experiment is shown in Fig. S1 and S2.† The requirement for a cell to be considered "adherent" was a length 1.3 times its width.

Adherent morphology was confirmed by comparing cell behavior in the trapping structure to cells cultured under

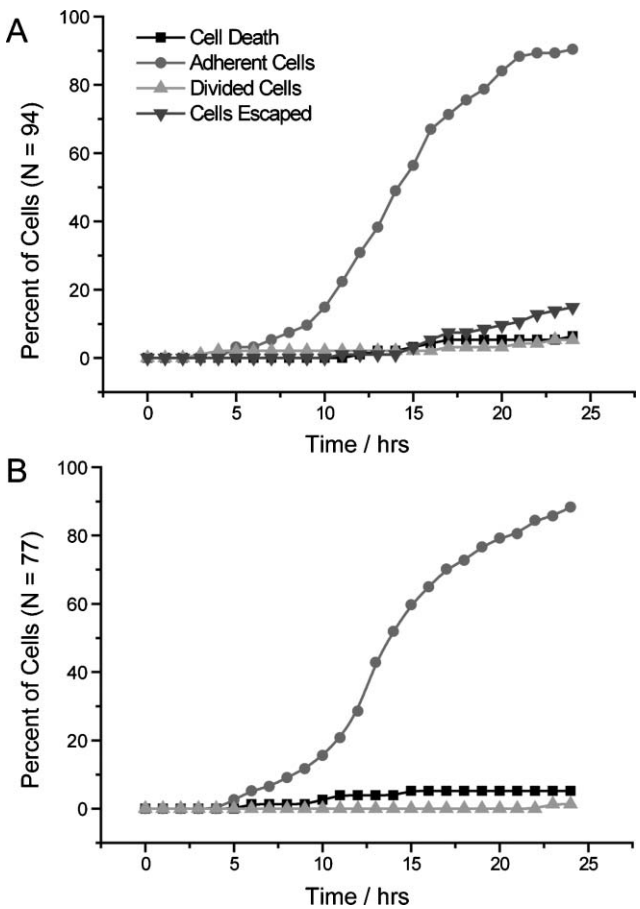

Fig. 5 Cell behavior in trapping structures and the control substrate. (A) Cell adhesion, division, and death are reported every hour for individual cells in the single cell array. (B) The same characteristics are plotted for culture on a control glass slide without perfusion.

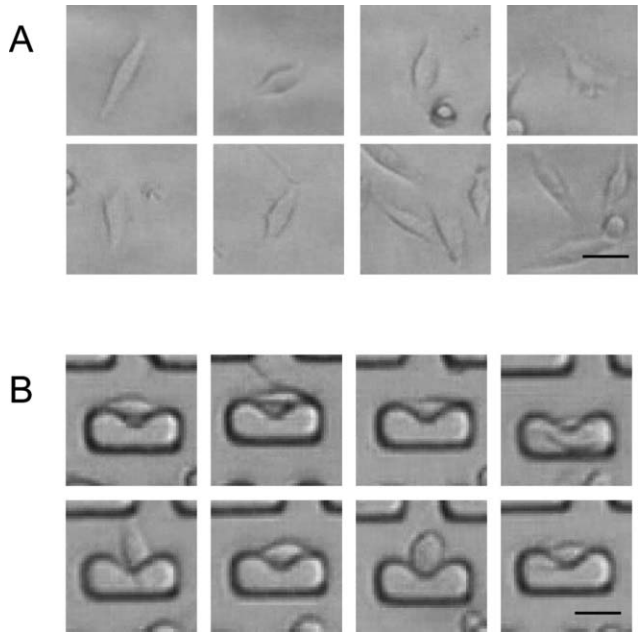

Fig. 6 Morphology in trapping structures and control substrate. HeLa cell morphology is shown after 24 hour growth on a glass substrate without perfusion (A) and after 24 hours of perfusion in the trapping array (B). Notice the similar adherent morphology. Some differences are observed due to attachment of cells to the PDMS structures in (B). Scale bars are 25 μm.

similar conditions in the control experiment (Fig. 6). Similar adherent and elongated morphology is observed in the images seen on a glass slide (Fig. 6A) and in the device (Fig. 6B).

Conclusions

We have demonstrated a microfluidic-based hydrodynamic trapping method for creating arrays of single adherent cells with dynamic control of perfusion possible. HeLa cells are cultured and a high level of maintenance in the original position of trapping is observed after 24 hours. Additionally, cell division, adhesion, and apoptotic behavior was comparable to static culture on the same substrate, indicating cells are not stressed above normal culture conditions. After cell division, daughter cells were also observed to be maintained within the original trapping structure. As compared with previous single cell arrays, cell–cell communication by both contact and diffusible elements is a controllable parameter in this device. We anticipate this technique will be useful in single cell studies of metabolism, pharmacokinetics, drug toxicity, shear stress activation, and chemical signaling pathway activation and inhibition.

Acknowledgements

This research was supported by a Whitaker Foundation graduate fellowship (D. D.), Intel Research Fund, and Taiwan Merit Scholarship TMS-094-2-A-008 (L.W.). All master copies for PDMS molding were fabricated in the UC Berkeley microfabrication facility.

References

1 C. V. Rao, D. M. Wolf and A. P. Arkin, *Nature*, 2002, **420**, 231–237.
2 M. E. Lidstrom and D. R. Meldrum, *Nat. Rev. Microbiol.*, 2003, **1**, 158–164.
3 A. Khademhosseini, R. Langer, J. Borenstein and J. P. Vacanti, *Proc. Natl. Acad. Sci. U. S. A.*, 2006, **103**, 2480–2487.
4 A. Prokop, Z. Prokop, D. Schaffer, E. Kozlov, J. Wikswo, D. Cliffel and F. Baudenbacher, *Biomed. Microdevices*, 2004, **6**, 325–339.
5 S. Petronis, M. Stangegaard, C. B. V. Christensen and M. Dufva, *Biotechniques*, 2006, **40**, 368–376.
6 C. J. Wei, X. Xu and C. W. Lo, *Annu. Rev. Cell Dev. Biol.*, 2004, **20**, 811–838.
7 A. Rustom, R. Saffrich, I. Markovic, P. Walther and H. H. Gerdes, *Science*, 2004, **303**, 1007–1010.
8 J. P. Himanen and D. B. Nikolov, *Trends Neurosci.*, 2003, **26**, 46–51.
9 M. Thery, V. Racine, A. Pepin, M. Piel, Y. Chen, J. B. Sibarita and M. Bornens, *Nat. Cell Biol.*, 2005, **7**, 947–U929.
10 C. H. Thomas, J. H. Collier, C. S. Sfeir and K. E. Healy, *Proc. Natl. Acad. Sci. U. S. A.*, 2002, **99**, 1972–1977.
11 A. Tourovskaia, T. Barber, B. T. Wickes, D. Hirdes, B. Grin, D. G. Castner, K. E. Healy and A. Folch, *Langmuir*, 2003, **19**, 4754–4764.
12 M. Veiseh, B. T. Wickes, D. G. Castner and M. Q. Zhang, *Biomaterials*, 2004, **25**, 3315–3324.
13 J. L. Tan, W. Liu, C. M. Nelson, S. Raghavan and C. S. Chen, *Tissue Eng.*, 2004, **10**, 865–872.
14 A. Revzin, P. Rajagopalan, A. W. Tilles, F. O. Berthiaume, M. L. Yarmush and M. Toner, *Langmuir*, 2004, **20**, 2999–3005.
15 E. Ostuni, R. Kane, C. S. Chen, D. E. Ingber and G. M. Whitesides, *Langmuir*, 2000, **16**, 7811–7819.
16 E. Ostuni, C. S. Chen, D. E. Ingber and G. M. Whitesides, *Langmuir*, 2001, **17**, 2828–2834.
17 A. Khademhosseini, S. Jon, K. Y. Suh, T. N. T. Tran, G. Eng, J. Yeh, J. Seong and R. Langer, *Adv. Mater.*, 2003, **15**, 1995–2000.
18 A. Folch and M. Toner, *Annu. Rev. Biomed. Eng.*, 2000, **2**, 227–256.
19 C. S. Chen, M. Mrksich, S. Huang, G. M. Whitesides and D. E. Ingber, *Science*, 1997, **276**, 1425–1428.
20 M. C. Berg, S. Y. Yang, P. T. Hammond and M. F. Rubner, *Langmuir*, 2004, **20**, 1362–1368.
21 X. Y. Jiang, R. Ferrigno, M. Mrksich and G. M. Whitesides, *J. Am. Chem. Soc.*, 2003, **125**, 2366–2367.
22 B. M. Taff and J. Voldman, *Anal. Chem.*, 2005, **77**, 7976–7983.
23 J. R. Rettig and A. Folch, *Anal. Chem.*, 2005, **77**, 5628–5634.
24 M. Tanase, E. J. Felton, D. S. Gray, A. Hultgren, C. S. Chen and D. H. Reich, *Lab Chip*, 2005, **5**, 598–605.
25 P. J. Hung, P. J. Lee, P. Sabounchi, R. Lin and L. P. Lee, *Biotechnol. Bioeng.*, 2005, **89**, 1–8.
26 P. J. Hung, P. J. Lee, P. Sabounchi, N. Aghdam, R. Lin and L. P. Lee, *Lab Chip*, 2005, **5**, 44–48.
27 G. M. Walker, H. C. Zeringue and D. J. Beebe, *Lab Chip*, 2004, **4**, 91–97.
28 J. W. Song, W. Gu, N. Futai, K. A. Warner, J. E. Nor and S. Takayama, *Anal. Chem.*, 2005, **77**, 3993–3999.
29 W. Gu, X. Y. Zhu, N. Futai, B. S. Cho and S. Takayama, *Proc. Natl. Acad. Sci. U. S. A.*, 2004, **101**, 15861–15866.
30 N. Futai, W. Gu, J. W. Song and S. Takayama, *Lab Chip*, 2006, **6**, 149–154.
31 L. Kim, M. D. Vahey, H. Y. Lee and J. Voldman, *Lab Chip*, 2006, **6**, 394–406.
32 A. Tourovskaia, X. Figueroa-Masot and A. Folch, *Lab Chip*, 2005, **5**, 14–19.
33 S. W. Rhee, A. M. Taylor, C. H. Tu, D. H. Cribbs, C. W. Cotman and N. L. Jeon, *Lab Chip*, 2005, **5**, 102–107.
34 A. M. Taylor, M. Blurton-Jones, S. W. Rhee, D. H. Cribbs, C. W. Cotman and N. L. Jeon, *Nat. Methods*, 2005, **2**, 599–605.
35 D. Di Carlo, N. Aghdam and L. P. Lee, *Anal. Chem.*, 2006, **78**, 4925–4930.
36 D. Di Carlo, C. Ionescu-Zanetti, Y. Zhang, P. Hung and L. P. Lee, *Lab Chip*, 2005, **5**, 171–178.
37 S. Li, N. F. Huang and S. Hsu, *J. Cell. Biochem.*, 2005, **96**, 1110–1126.
38 L. G. Griffith and M. A. Swartz, *Nat. Rev. Mol. Cell Biol.*, 2006, **7**, 211–224.